Received: 27 November 2023 | Revised: 22 October 2024 | Accepted: 25 October 2024

DOI: 10.1111/nan.13016

ORIGINAL ARTICLE

Neuropathology and Applied Neurobiology
JOURNAL OF THE BRITISH NEUROPATHOLOGICAL SOCIETY

WILEY

Microglia induce an interferon-stimulated gene expression profile in glioblastoma and increase glioblastoma resistance to temozolomide

Mia Dahl Sørensen[1,2] | Rikke Frydendahl Sick Olsen[1] | Mark Burton[3,4] | Stephanie Kavan[2,3] | Stine Asferg Petterson[1,2] | Mads Thomassen[3,4] | Torben Arvid Kruse[3,4] | Morten Meyer[5,6] | Bjarne Winther Kristensen[1,2,7,8]

[1]Department of Pathology, Odense University Hospital, Odense, Denmark

[2]Department of Clinical Research, University of Southern Denmark, Odense, Denmark

[3]Department of Clinical Genetics, Odense University Hospital, Odense, Denmark

[4]Clinical Genome Center, Department of Clinical Research, University of Southern Denmark, Odense, Denmark

[5]Department of Neurobiology Research, Institute of Molecular Medicine, University of Southern Denmark, Odense, Denmark

[6]Brain Research Inter-Disciplinary Guided Excellence (BRIDGE), Department of Clinical Research, University of Southern Denmark, Odense, Denmark

[7]Department of Pathology, The Bartholin Institute, Rigshospitalet, Copenhagen University Hospital, Copenhagen, Denmark

[8]Department of Clinical Medicine and Biotech Research & Innovation Centre (BRIC), University of Copenhagen, Copenhagen, Denmark

Correspondence
Mia Dahl Sørensen, Department of Pathology, Odense University Hospital, J.B. Winsløws Vej 15, 5000, Odense, Denmark.
Email: mia.soerensen@rsyd.dk

Funding information
This work was supported by The Danish Medical Research Council (4183-00183), Novo Nordisk Foundation (NNF19OC0058427), Odense University Hospital Research Funds, University of Southern Denmark, The Danish Cancer Society, Oda and Hans Svenningsen's Foundation, Krista and Viggo Petersen Foundation, and Brødrene Hartmann's Foundation.

Abstract

Aims: Glioblastoma is the most malignant primary brain tumour. Even with standard treatment comprising surgery followed by radiation and concomitant temozolomide (TMZ) chemotherapy, glioblastoma remains incurable. Almost all patients with glioblastoma relapse owing to various intrinsic and extrinsic resistance mechanisms of the tumour cells. Glioblastomas are densely infiltrated with tumour-associated microglia and macrophages (TAMs). These immune cells affect the tumour cells in experimental studies and are associated with poor patient survival in clinical studies. The aim of the study was to investigate the impact of microglia on glioblastoma chemo-resistance.

Methods: We co-cultured patient-derived glioblastoma spheroids with microglia at different TMZ concentrations and analysed cell death. In addition, we used RNA sequencing to explore differentially expressed genes after co-culture. Immunostaining was used for validation.

Results: Co-culture experiments showed that microglia significantly increased TMZ resistance in glioblastoma cells. RNA sequencing revealed upregulation of a clear interferon-stimulated gene (ISG) expression signature in the glioblastoma cells after co-culture with microglia, including genes such as *IFI6*, *IFI27*, *BST2*, *MX1* and *STAT1*. This ISG expression signature is linked to STAT1 signalling, which was confirmed by immunostaining. The ISG expression profile observed in glioblastoma cells with enhanced TMZ resistance corresponded to the interferon-related DNA damage resistance signature (IRDS) described in different solid cancers.

Conclusions: Here, we show that the IRDS signature, linked to chemo-resistance in other cancers, can be induced in glioblastoma by microglia. ISG genes and the microglia inducing the ISG expression could be promising novel therapeutic targets in glioblastoma.

KEYWORDS
chemo-resistance, glioblastoma, interferon, microglia, STAT

INTRODUCTION

Glioblastoma is the most frequent and malignant primary brain tumour in adults. For almost two decades, standard therapy has consisted of surgery followed by radiotherapy as well as concomitant and adjuvant chemotherapy with temozolomide (TMZ) [1]. Despite extensive treatment, the median survival is less than 15 months, and the 5-year survival is below 5% [2]. Glioblastomas nearly always recur because of their infiltrative growth preventing complete resection, as well as their ability to circumvent the cytotoxic effects of treatment. One of the most well-described tactics involves the profitable exploitation of the DNA repair enzyme O^6-methylguanine-DNA methyltransferase (MGMT). In non-neoplastic cells, MGMT acts as a DNA repair enzyme protecting cells from apoptosis by removing alkyl groups from the O6 position on guanine. In glioblastoma, MGMT enables the tumour cells to evade the alkylating and thus apoptotic effect of TMZ [3]. Methylation of the MGMT promoter silences the gene leading to increased chemo-sensitivity and is associated with prolonged survival in glioblastoma patients [4, 5]. Thus, TMZ has an effect on tumours with methylated MGMT promoters [6], which account for ~50% of all glioblastomas [7], and for these tumours, the resistance mechanisms are less clear. Alternative resistance mechanisms may involve the tumour microenvironment, in particular, the microglia and macrophages, which are recruited to the site of the tumour. These immune cells constitute up to 30%–50% of the total tumour [8–11] and secrete factors that affect the tumour cells in various ways [12]. Subsets of tumour-associated microglia and macrophages (TAMs) have been linked to poorer patient survival in glioblastoma, such as $CD163^+$ TAMs [13] and $CD204^+$ TAMs [11] as previously reported by our group. In addition, subsets of TAMs are involved in radio-resistance of glioblastomas [14–16] and may also be implicated in chemo-resistance [17]. Mechanisms for this chemo-resistance have been suggested in small pre-clinical studies with commercial and patient-derived cell lines, proposing that microglial secretion of the complement component C5a may facilitate DNA damage repair in glioblastoma [18], or that A Disintegrin and Metalloproteinase Domain 8 (ADAM8)-recruited macrophages may be involved in TMZ resistance [19]. However, the challenge of TMZ resistance in glioblastoma remains to be solved.

Interferon (IFN)/signal transducer and activator of transcription 1 (STAT1) signalling in tumour cells leads to expression of an IFN-stimulated gene (ISG) expression profile with high expression of genes, such as *IFI27*, *BST2*, *MX1*, *OAS1*, *IFIT1* and *STAT1* [20]. In normal cells, the ISGs are involved in antiviral responses, but high ISG expression has been identified in many different cancer types in a comprehensive pan-cancer study describing transcriptional intratumour heterogeneity [21]. The ISG expression profile has been linked to increased glioblastoma stemness [22], resistance to immune checkpoint blockade in melanoma [23] and radiation and chemotherapy resistance in breast cancer [24]. Accordingly, Weichselbaum *et al.* defined the ISG signature as an IFN-related DNA damage resistance signature (IRDS) and demonstrated the presence of this signature in lung, prostate, head and neck cancers, as well as high-grade gliomas [24]. The IRDS signature was recently identified in a subpopulation of tumour cells in glioblastoma, where it was found to correlate with poorer survival [25].

Key Points

- Microglia increase TMZ resistance in glioblastoma.
- Microglia induce an interferon-stimulated gene expression profile in glioblastoma cells.
- The microglial-induced interferon-stimulated gene expression profile is mediated by STAT1 signalling.

In this study, we report a pronounced microglial-induced protection from TMZ in glioblastoma using an experimental *in vitro* set-up. Patient-derived glioblastoma spheroids co-cultured with microglia upregulate the IRDS gene expression profile making them less responsive to TMZ treatment. This suggests that microglia may contribute to chemo-resistance by inducing the IRDS profile in glioblastoma cells.

MATERIALS AND METHODS

Cell cultures

Patient-derived glioblastoma spheroid cultures (T78, T87, T105, T110, T116 and T121) were established in our lab as previously described [26–29] and cultured as free-floating spheroids in serum-free Neurobasal-A medium (Gibco, NY, USA) supplemented with 1% B27 (Invitrogen, MA, USA), 0.5% N2 (Invitrogen), 1% L-Glutamine (Gibco), 1% penicillin/streptomycin (Gibco), 25-ng/mL EGF (Sigma-Aldrich, MO, USA) and 25-ng/mL bFGF (PeproTech, NJ, USA). Written informed consent was obtained from all patients, and the Regional Scientific Ethical Committee and the Data Protection Authority approved the study. All glioblastoma spheroid cultures have previously been thoroughly characterised and validated by spheroid formation and differentiation assays, molecular subtyping according to Verhaak et al. [30], sequencing with a custom next-generation sequencing panel for the mutational status of 20 of the most frequently mutated genes in glioma [31], and by orthotopic xenograft implantation in mice. **Table** S1 provides an overview of the characteristics of the patient-derived glioblastoma spheroids used in the study. All spheroid cultures had methylated MGMT promoter and were derived from glioblastomas, isocitrate dehydrogenase (IDH) wildtype. The mouse BV2 immortalised microglia cell line [32, 33] (AcceGen Biotech, NJ, USA) was maintained in RPMI 1640 Medium with GlutaMAX™ (Gibco) supplemented with 5% foetal bovine serum (FBS) (Sigma-Aldrich) and 1% penicillin/streptomycin. The human SV40 immortalised microglia cell line [29, 34] (cat. no. T0251, Applied biological materials, BC, Canada) and human primary microglia (cat. no. 37089-01, Celprogen, CA, USA) were grown adherently in

collagen-coated (Type I solution from rat tail, Sigma Aldrich) flasks with DMEM (high glucose, GlutaMAX) medium (Gibco) supplemented with 10% FBS and 1% penicillin/streptomycin. Microglia cell culture medium was switched to serum-free Neurobasal-A medium 24 h before all experiments. All cells were cultured at 37°C in a standard tissue culture incubator (95% humidity, 95% atmospheric air, 5% CO_2).

Co-culture experiments

Co-culture experiments were carried out to investigate the influence of microglia on the effect of TMZ in glioblastoma spheroids. For each glioblastoma spheroid culture, we determined the optimal time point for the co-culture experiments based on TMZ response (**Figure** S1) and spheroid size to avoid large areas of central necrosis in big individual spheroids.

For direct co-culturing, BV2 immortalised microglia were seeded onto 24-well plates (15,000 cells/well) and allowed to attach. Thereafter, media and non-attached cells were replaced with fresh media and single glioblastoma spheroids were carefully pipetted into the wells (∼10–15 spheroids/well) with or without BV2 microglia followed by 24 h of incubation. Next, cultures were treated with TMZ (Sigma-Aldrich) dissolved in dimethyl sulfoxide (DMSO, Sigma-Aldrich) and diluted in serum-free media to a final concentration of 60 or 120 μM for 24 h. DMSO was used as a negative control.

For indirect co-culturing, hanging cell culture inserts with a pore size of 1.0 μm for 24-well plates were used (Millicell®, cat. no. MCRP24H48, Millipore, MA, USA). BV2 immortalised microglia (15,000 cells/insert), SV40 immortalised microglia (45,000 cells/insert) or primary microglia (15,000 cells/insert) were plated onto the inserts. Single glioblastoma spheroids were pipetted into the lower chamber of the wells. Inserts with or without microglia were placed in the wells. Cells were allowed to (co)-incubate for 24 h and then treated with TMZ for 24–72 h.

Microglia-conditioned medium (MCM) was generated as follows: BV2 immortalised microglia were seeded onto 24-well plates (15,000 cells/well) and allowed to attach. Media and non-attached cells were replaced with fresh medium, and cells were incubated for 24 h and then treated with TMZ or DMSO for 24 h. Microglia supernatants were harvested and transferred into 24-well plates. Control medium (COM) was prepared similarly to the MCM but without the presence of microglia. Single glioblastoma spheroids were pipetted into the wells containing either MCM or COM, allowed to incubate for 24 h and then treated with TMZ or DMSO for 24–48 h.

Propidium iodide fluorescence assay

Cell death was visualised using propidium iodide (PI) (Sigma-Aldrich) [35]. PI was added to the cell cultures to a final concentration of 2 μM and incubated for 3–4 h at 37°C. Greyscale fluorescence images were acquired by a Leica DM IRB inverted fluorescence microscope equipped with a standard rhodamine filter and a Leica DFC300 FX camera. The PI intensity of individual spheroids, BV2 immortalised and SV40 immortalised microglia was measured using ImageJ software (NIH) [36].

Lactate dehydrogenase activity

The cytotoxic effect of TMZ on microglia was assessed by measuring the lactate dehydrogenase (LDH) activity released by microglia into the supernatant using a colourimetric LDH assay (cat. no. 11644793001, Roche, Sigma-Aldrich). Briefly, microglia were seeded onto uncoated (BV2) or collagen-coated (SV40 and primary microglia) 24-well plates in serum-free medium with 15,000 cells/well (BV2 and primary microglia) or 45,000 cells/well (SV40 microglia). After 24 h, TMZ (0–960 μM) was added into each well, and cells were exposed for 48 h. The cell supernatants were then harvested and transferred into 96-well plates. The LDH reagent was added (1:1) and allowed to incubate for 30 min at room temperature, and optical densities were measured at 490 and 630 nm using an ELISA reader.

Cell viability/proliferation assay

Microglia viability following TMZ exposure was examined using the colourimetric WST-1 based assay (cat. no. 11644807001, Roche, Sigma-Aldrich). Microglia were seeded onto uncoated (BV2 microglia) or collagen-coated (SV40 and primary microglia) 96-well plates in serum-free medium with 2,500 cells/well (BV2 microglia and primary microglia) or 7,500 cells/well (SV40 microglia). After 24 h, TMZ (0–960 μM) was added. Cells were exposed for 48 h. The supernatant was then discarded and replaced by fresh medium and WST-1 (1:10) followed by an incubation time of 3 h at 37°C. Optical densities were measured at 450 and 630 nm using an ELISA reader.

Immunohistochemistry and quantitative image analysis

Glioblastoma spheroids were fixed in 10% neutral-buffered formalin for 24 h. Fixed spheroids were washed three times with 0.9% NaCl and clotted with a mix of thrombin/plasma followed by embedment in paraffin. Three micrometre sections were then mounted on FLEX IHC slides (Dako, Glostrup, Denmark). Immunostaining with unconjugated primary rabbit monoclonal antibodies against cleaved caspase-3 (clone 5A1E, Cell Signaling Technology, MA, USA) and p-STAT1 (clone D3B7, Cell Signaling Technology) was performed semi-automatically using the Dako Autostainer Link 48 instrument and EnVision FLEX+ detection system (Agilent Technologies, CA, USA). Following deparaffinisation, rehydration, heat-induced epitope retrieval in TEG (10-mmol/L Trisbase and 0.5-mmol/L EGTA, pH 9) for 15 min and blocking of endogenous peroxidase, sections were incubated with anti-cleaved caspase-3 (1:400) or p-STAT1 (1:800) for

60 min at room temperature. The antigen–antibody complex was detected using EnVision FLEX+ with DAB as chromogen. Immunostaining with primary rabbit monoclonal antibodies against STAT1 (clone D1K9Y, Cell Signaling Technology), bone marrow stromal cell antigen 2 (BST2) (clone E4N3W, Cell Signaling Technology) and myxovirus resistance protein 1 (MX1) (clone D3W7I, Cell Signaling Technology) was carried out on the fully-automated DISCOVERY ULTRA immunostainer (Ventana Medical Systems, Inc., AZ, USA). Standard protocols included epitope retrieval in protease-3 for 4 min followed by cell conditioning 1 buffer for 32 min at 100°C (STAT1) or cell conditioning 1 buffer for 32 min at 100°C followed by protease-3 for 4 min (BST2 and MX1), quenching of endogenous peroxidase and incubation with anti-STAT1 (1:800), anti-BST2 (1:400) or anti-MX1 (1:50) for 32 min at 36°C. The bound antigen–antibody complex was visualised with OptiView-DAB according to the manufacturer's instructions. Sections were counterstained with Mayers haematoxylin or Haematoxylin II plus bluing reagent, and coverslips were mounted using Pertex® Mounting Medium (HistoLab Products AB, Göteborg, Sweden). Stained slides were digitalised using the NanoZoomer 2.0HT whole slide scanner (Hamamatsu Photonics) equipped with a 40× objective. Images were then imported into the Visiopharm Image Analysis Software (Visiopharm, Hørsholm, Denmark), version 2018.4, and pixel-based algorithms were designed as previously described [37] to quantify fractions of the positive staining area within the individually outlined glioblastoma spheroids.

RNA isolation, sequencing and data analyses

Indirect co-culturing was performed with the SV40 immortalised microglia cell line and the glioblastoma spheroid culture T121, and the co-cultures were exposed to 60 or 120 μM TMZ for 48 h using DMSO as negative control, as described above. T121 spheroids were harvested from the 24-well plates, centrifuged and stored as dry pellets. Dry pellets of single cultures of T121 spheroids were prepared in a similar manner. The experiment was performed in biological triplicates, and all samples were stored at −80°C until RNA extraction and sequencing. Total RNA was isolated using the RNeasy Mini Kit (Qiagen, Venlo, The Netherlands) according to the manufacturer's protocol, and sample RNA concentration was measured with NanoDrop™ 2000 (Thermo Scientific, MA, USA). RNA sequencing (RNA-seq) was performed using the Illumina NextSeq sequencer and 2 × 75 bp paired-end reads. The raw data (BCL files) were first demultiplexed using Illumina software CASAVA thereby creating FASTQ files. The FASTQ files were processed using (BBDUK) from the BBTools package [38] for trimming remnant adaptor sequences, removal of low-quality bases and reads, and kmer-filtering. The quality filtered reads were subsequently first aligned against the human transcriptome (Homo_sapiens.GRCh38.95) and then to the human genome (GRCh37/hg19) using TOPHAT2 [39]. Quantification was done using the HTseq-count Python module embedded in the HTSeq tool package [40]. The *edgeR* R-package [41] was used for the transformation of the raw counts into counts per million (cpm) and for the filtration of very low expressed genes. Only genes that had cpm ≥ 1 in at least three samples were kept for further analysis. This step led to a total of 15,128 genes for further downstream analysis. After filtering, the data were normalised using Trimmed Mean of *M*-values (TMM) normalisation. For differential expression analysis, the glmFit and glmLRT functions embedded in the *edgeR* R package were used, and the false discovery rate (FDR) was applied to correct for multiple testing. Genes having an FDR ≤ 0.05 were considered significantly differentially expressed.

Gene set enrichment analysis

Gene Set Enrichment Analysis (GSEA) [42] was performed using the GSEA software v.3.0 to determine if a given set of curated genes/pathways showed statistically significant concordant differences between the above-compared groups. The GSEA was run on pre-ranked individual genes (based on log2 fold changes and considering all past-filtering expressed genes). The collection of human KEGG (Kyoto Encyclopedia of Genes and Genomes, http://www.genome.jp/kegg/) and Reactome (https://reactome.org/) defined gene sets were used as input for the analysis. Next, an enrichment score was calculated for each of these *a priori*-defined gene sets, which is a metric of how significantly the members of a gene set deviate from a randomly distributed ordered list compared with the input pre-ranked list. In our analysis, GSEA was conducted using 1,000 permutations, and minimum and maximum gene sets size was set to 15 and 500, respectively. Gene sets with an FDR ≤ 0.05 were considered to be statistically significantly enriched between groups.

Correlation analyses between microglia markers and ISGs in TCGA and CGGA data

The Chinese Glioma Genome Atlas (CGGA) RNA-seq data were downloaded from the GlioVis web application (http://gliovis.bioinfo.cnio.es) [43] and filtered to exclude IDH-mutant, 1p19q-codeleted and secondary glioblastomas as well as patients with an age of <18 years. Both primary and recurrent glioblastoma patients were included. In addition, The Cancer Genome Atlas (TCGA) microarray data (Agilent-4502A) from adult glioblastoma patients were downloaded from GlioVis and filtered to exclude IDH1-mutant and secondary glioblastomas. Both primary and recurrent glioblastoma patients were included.

Statistics

For the co-culture experiments, statistical analyses were performed with the GraphPad Prism software 5.0. Data were tested for normality and homogeneity of variance. Student's unpaired *t*-test or its non-parametric equivalent Mann–Whitney U-test was used for the comparison of two groups, whereas one-way ANOVA with

Bonferroni's correction or non-parametric Kruskal–Wallis test with Dunn multiple comparisons test was used when comparing more than two groups. Each experiment was performed as at least two independent biological replicates, and data were pooled from consecutive experiments and normalised using the means. For the correlation studies, statistical analyses were performed with the GraphPad Prism software 9.5. mRNA expression of selected ISGs (*IFI6*, *IF27*, *BST2*, *MX1*, *HERC6* and *STAT1*) and microglia markers (*AIF1* and *TMEM119*) were plotted against each other, and Pearson correlation coefficients (*r*) were calculated. *r* was used to test whether the relationship between the ISGs and microglia markers was significant using a two-tailed correlation analysis. $P < 0.05$ were considered statistically significant.

RESULTS

Microglia increase TMZ resistance of glioblastoma cells

Different co-culture experiments were performed to investigate the effect of microglia on TMZ sensitivity in glioblastoma cells (**Figure** 1A–C), analysing cell death with a PI assay. First, we selected a panel of glioblastoma cell cultures sensitive to TMZ treatment (**Figure** S1). Direct co-culture experiments (**Figure** 1A) of T87 and T78 glioblastoma spheroids and mouse BV2 immortalised microglia showed significantly reduced glioblastoma cell death after co-culture with microglia compared with cultures without microglia (**Figure** 1D–F). Next, we investigated whether the effect was caused by direct cell–cell contact or by secreted factors performing indirect co-culture experiments using transwell inserts that only permit the passage of secreted factors. Microglia were placed in the upper compartment, whereas the glioblastoma spheroids were placed in the bottom of the wells (**Figure** 1B). We observed the same effect as in the direct co-culture experiments; T87, T78 and T121 glioblastoma spheroids were significantly less sensitive to TMZ-induced cell death when cultured together with BV2 immortalised microglia in the transwell insert (**Figure** 1G–I). To further explore this, glioblastoma spheroids were exposed to TMZ in the presence and absence of microglia-conditioned medium (**Figure** 1C). BV2 immortalised microglia were cultured with and without TMZ and, after 24 h, the microglia-conditioned medium was harvested and transferred to glioblastoma spheroid cultures that were then exposed to different concentrations of TMZ. We observed significantly reduced glioblastoma cell death when cultured in microglia-conditioned medium treated with 0 and 60 μM TMZ (**Figure** 1J–L). However, when microglia had been exposed to 120 μM TMZ, we did not see a significant protective effect.

To investigate the human microglial effect on TMZ sensitivity, the indirect co-culture experiments were repeated using the human SV40 immortalised microglia cell line. Comparably with the mouse BV2 immortalised microglia, we observed significantly reduced glioblastoma spheroid death when co-culturing six different glioblastoma spheroid cultures with SV40 immortalised microglia (**Figure** 2A–F). Next, we analysed glioblastoma cell death by immunohistochemical staining (IHC) of cleaved caspase-3, an apoptotic marker, using the indirect co-cultures (**Figure** 2G). We observed a significant microglial-induced reduction in cleaved caspase-3 expression in two different glioblastoma spheroid cultures (**Figure** 2H,I). To further verify the protective effect of microglia, we performed indirect co-culture experiments with two glioblastoma spheroid cultures using human primary microglia that more closely resemble the microglia observed *in vivo*, and here, we observed a significantly reduced cell death in the co-cultured glioblastoma spheroids (**Figure** 2J,K). To investigate the influence of TMZ on microglia, we performed cell death/viability assays on the three microglia cell lines, and these experiments showed a significant cytotoxic effect only at high TMZ concentrations (≥480 μM for cell death and ≥240 μM for cell viability) (**Figure** S2).

In summary, we discovered that both mouse and human immortalised microglia, as well as human primary microglia, secrete factors that reduce TMZ-mediated cell death and leave glioblastoma cells unresponsive or less responsive to TMZ.

Microglia induce an interferon-stimulated gene expression profile in glioblastoma cells

To gain more insight into why glioblastoma cells become resistant to TMZ after co-culture with microglia, we performed RNA-seq on T121 glioblastoma spheroids cultured with or without human SV40 immortalised microglia. We performed indirect co-culturing to avoid cross-contamination with microglia. After filtering and normalisation of the RNA-seq data, differential gene expression analysis and GSEA were performed.

First, differential gene expression between T121 spheroids exposed to 0 μM or 60/120 μM TMZ was investigated. As expected, we observed an upregulation of pro-apoptotic factors (e.g., *FAS*, *PMAIP1*, *TNFRSF10A*, *CHAC1* and *TRIB3*) and the cell cycle inhibitor *CDKN1A*. GSEA supported this, as it showed upregulation of the KEGG p53 signalling pathway as well as the KEGG apoptosis (**Figure** 3A). Next, the microglial impact on glioblastoma spheroids was examined. We analysed differentially expressed genes between T121 spheroids cultured alone or co-cultured with microglia. We observed a clear ISG expression profile in the glioblastoma spheroids co-cultured with microglia, with a high number of upregulated ISGs (e.g., *IFI27*, *MX1*, *BST2*, *IFI6*, *HERC6* and *STAT1*) (**Figure** 3B). GSEA REACTOME and KEGG analyses indicated IFN and JAK/STAT signalling, respectively. An almost identical gene expression profile was identified when comparing T121 spheroids cultured alone with T121 spheroids co-cultured with microglia and treated with TMZ. Multiple ISGs were upregulated, and GSEA analysis revealed IFN and JAK/STAT signalling (**Figure** 3C). The differential expression of selected ISGs is illustrated in a heatmap in **Figure** 4A (see **Tables** 1 and S2 for the top 25 or top 100 differentially expressed genes and the supplementary Excel data file (**Data S1**) for raw expression with annotations). The heatmap includes some of the most described ISGs in the literature and compares the gene expression in T121 single-

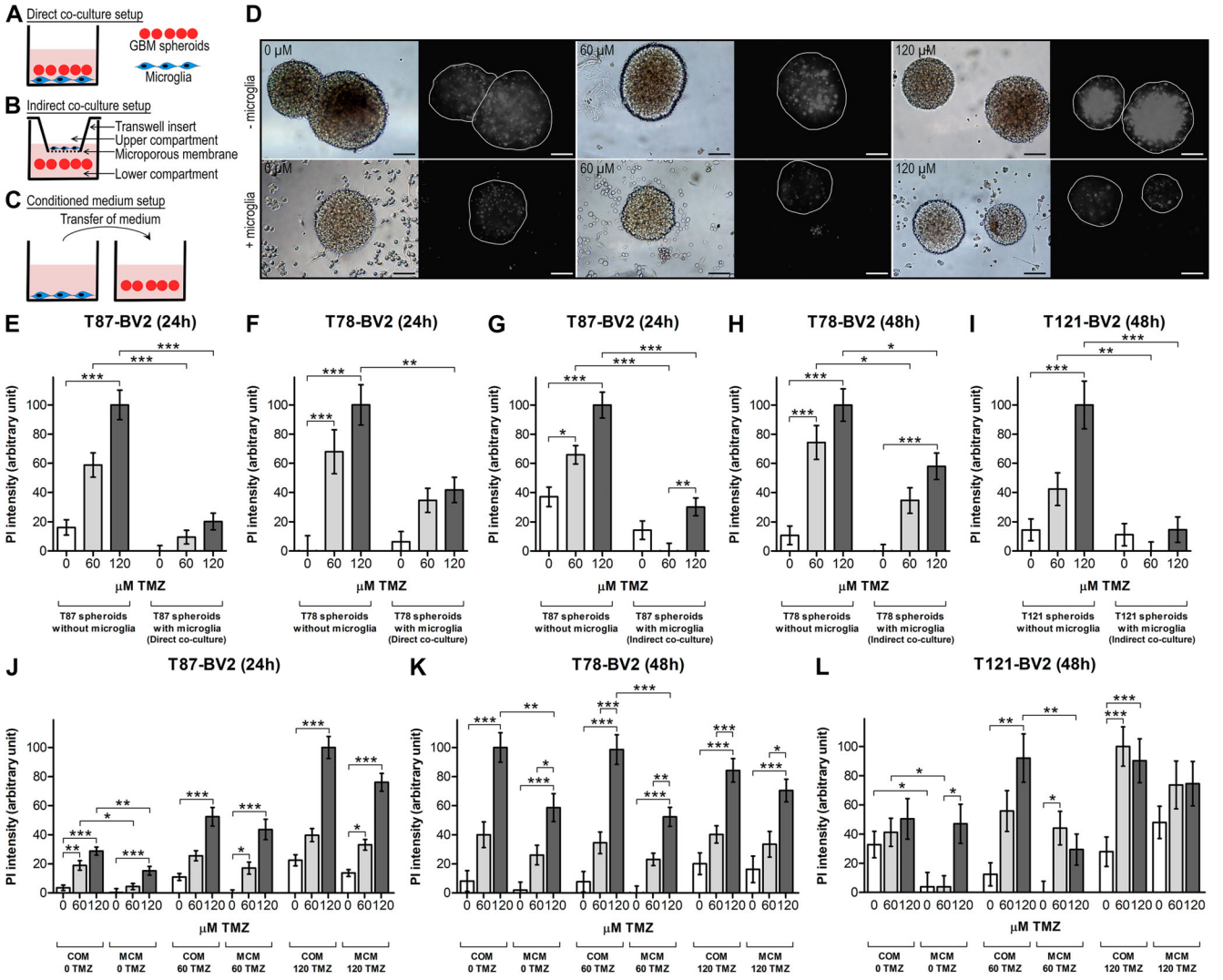

FIGURE 1 Mouse BV2 immortalised microglia reduce TMZ sensitivity of glioblastoma spheroids. (**A–C**) Illustration of culture set-ups showing direct co-culture of microglia and glioblastoma (GBM) spheroids (A), indirect co-culture with GBM spheroids and microglia separated by a microporous membrane (B) and a set-up where GBM spheroids are treated with conditioned medium derived from microglia cultures (C). (**D**) Images of T87 spheroids cultured without (top) and with (bottom) BV2 microglia in a direct co-culture set-up with 0, 60 and 120 µM TMZ. The left panels show light microscope images of the spheroids, and the right panels indicate fluorescent microscope images of their respective propidium iodide (PI) signals (outlined using ImageJ). (**E, F**) Two spheroid cultures (T87 and T78) treated with TMZ showed reduced cell death (reduced PI intensity) after direct co-culture with BV2 microglia. (**G, H, I**) Three spheroid cultures (T87, T78 and T121) treated with TMZ showed reduced cell death after indirect co-culture with BV2 microglia. (**J, K, L**) Three spheroid cultures (T87, T78 and T121) treated with TMZ and control medium (COM, with and without TMZ) or BV2 microglia-conditioned medium (MCM, with and without TMZ). After 24 h (T87) or 48 h (T78 and T121) of culture, a significantly reduced TMZ-induced cell death of GBM spheroids was observed in MCM cultures treated with 0 or 60 µM TMZ, but not 120 µM TMZ. In figures J–L the TMZ concentrations right below the x-axis indicate TMZ in the culture, whereas the TMZ concentrations below the brackets indicate TMZ in the pre-treated COM and MCM cultures. The level of significance is indicated with asterisks (* $p < 0.05$; ** $p < 0.01$; *** $p < 0.005$). The standard error of the mean (SEM) based on at least two biological replicates is indicated by the vertical lines. The scale bar in D is 100 µm.

cultured spheroids with T121 co-cultured spheroids with and without TMZ exposure. All ISGs were significantly upregulated after co-culture with microglia, indicating that the ISG expression profile detected in our data is highly similar to the ISG expression profiles described in the literature. Collectively, microglia induced an ISG expression profile in glioblastoma cells, and the GSEA analysis suggested that JAK/STAT signalling may be involved.

The microglial-induced ISG expression profile is mediated by STAT1 signalling

Differential gene expression analysis as well as GSEA analysis on the RNA-seq data suggested the involvement of STAT1 signalling through upregulation of ISGs after co-culture with microglia. To confirm this, we performed immunostaining of STAT1 and phosphorylated (p-)

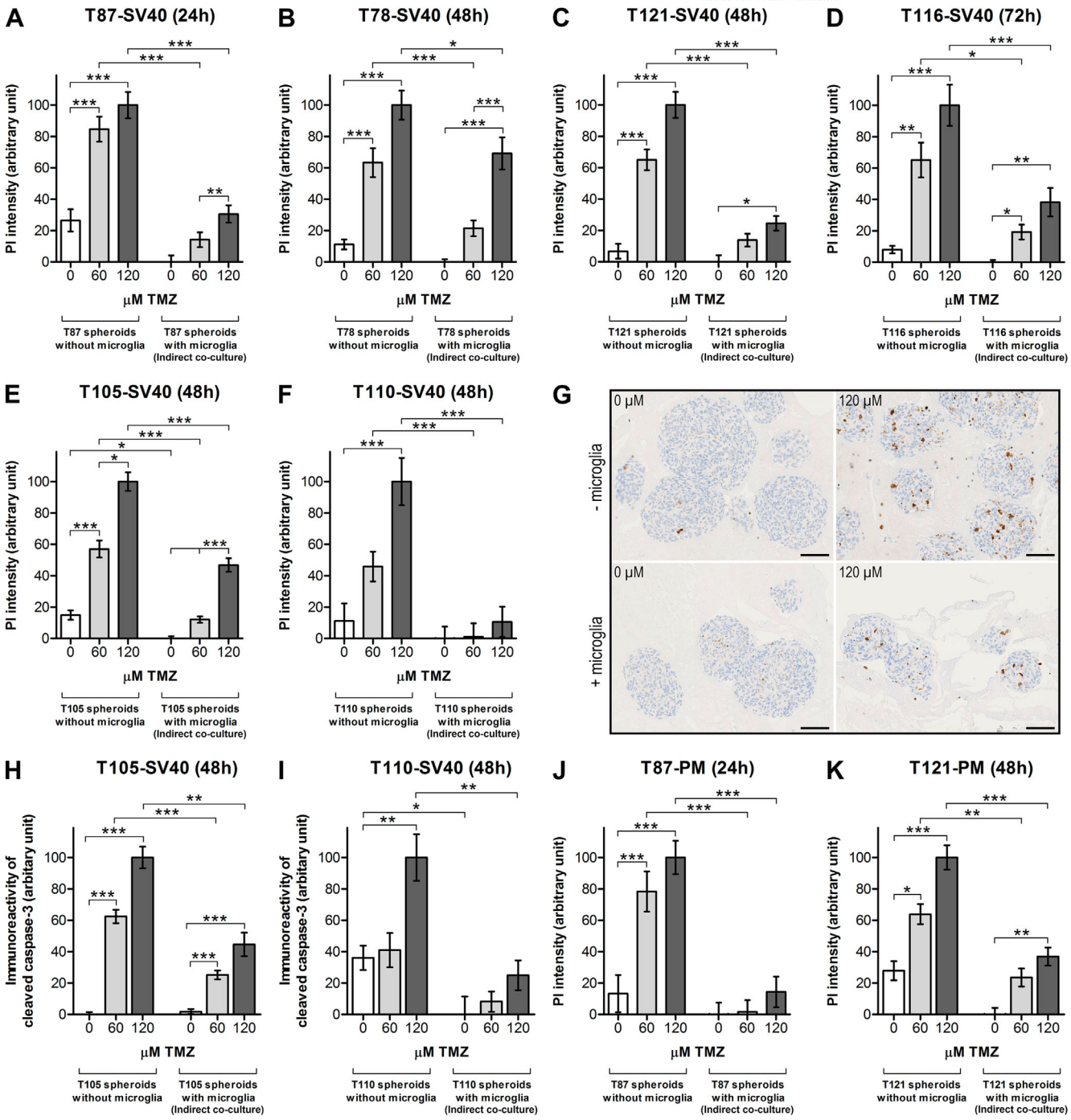

FIGURE 2 Human microglia increase TMZ resistance of glioblastoma spheroids. (**A–F**) Six glioblastoma spheroid cultures treated with TMZ showed significantly reduced cell death measured by PI intensity following indirect co-culture with human SV40 immortalised microglia. (**G**) IHC images of cleaved caspase-3 in spheroids cultured without (top) and with (bottom) SV40 microglia and treated with 0 (left) or 120 µM (right) TMZ, illustrated for T105. (**H, I**) Two spheroid cultures treated with TMZ showed significantly reduced apoptosis after indirect co-culture with SV40 microglia. (**J, K**) Two spheroid cultures treated with TMZ showed significantly reduced cell death after indirect co-culture with human primary microglia. The level of significance is indicated with asterisks (* $p < 0.05$; ** $p < 0.01$; *** $p < 0.005$). The SEM based on at least two biological replicates is indicated by vertical lines. The scale bar in G is 100 µm.

STAT1 as well as BST2 and MX1 on paraffin-embedded glioblastoma cell clots derived from indirect co-culture experiments with two glioblastoma spheroid cultures and SV40 immortalised microglia (**Figure** 4B). STAT1 and p-STAT1 were weakly expressed in T105 and T121 spheroids cultured alone but when co-cultured with microglia, STAT1 (**Figure** 4C,D) and p-STAT1 (**Figure** 4E,F) expression levels were significantly upregulated in both the presence and absence of TMZ. Similar results were found for BST2 (**Figure** 4G, H) and MX1

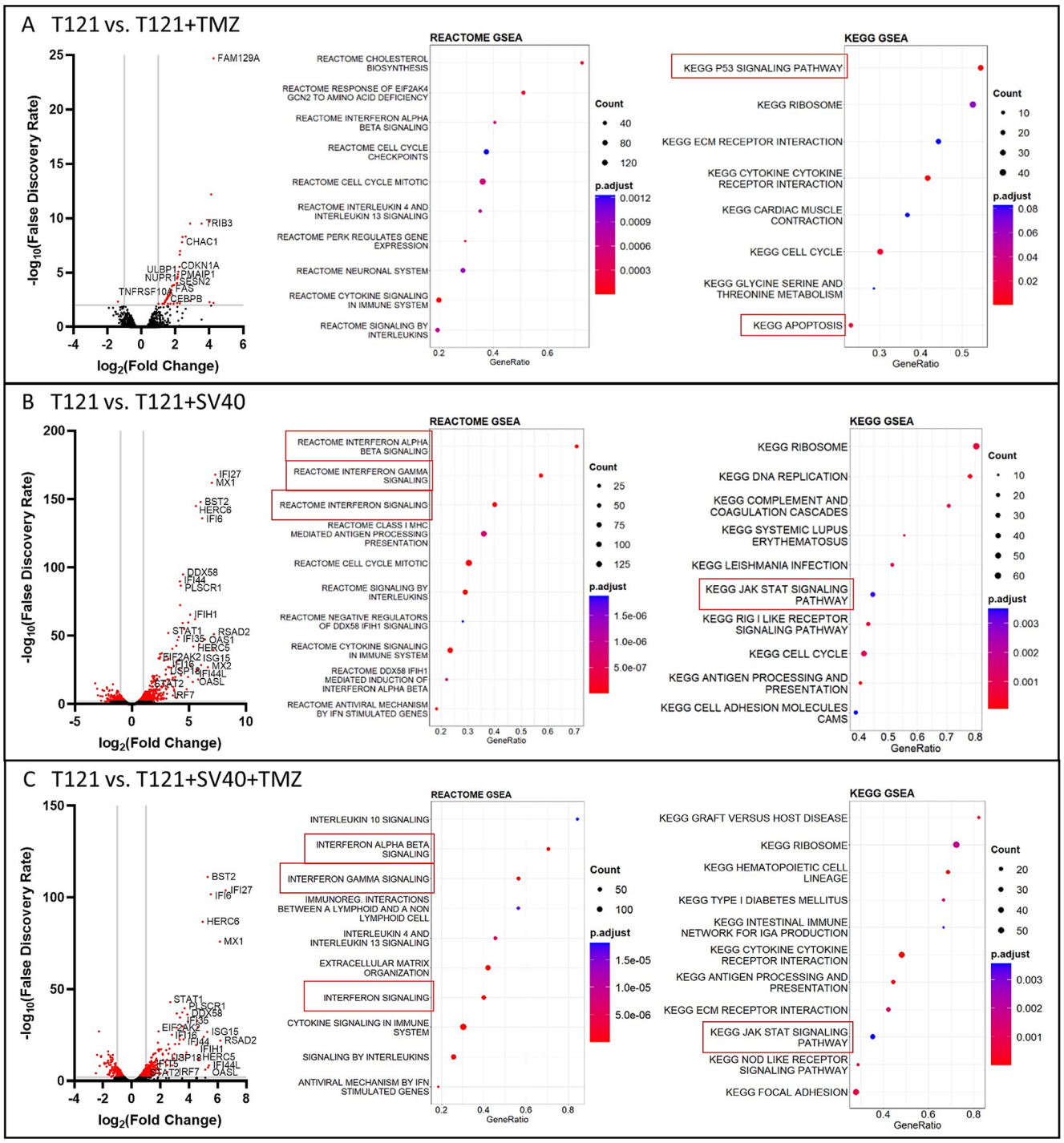

FIGURE 3 Glioblastoma spheroids acquire an ISG expression profile after co-culturing with microglia. We performed RNA-seq on TMZ-treated and non-treated T121 glioblastoma spheroids co-cultured with and without SV40 immortalised microglia. Differential gene expression analyses between different treatments are illustrated in volcano plots (left), and GSEA is shown (middle: REACTOME and right: KEGG). (**A**) Differential gene expression analysis between T121 spheroids cultured with and without TMZ showed induction of apoptosis after TMZ treatment. (**B**) Differential gene expression analysis between T121 spheroids cultured alone vs T121 spheroids cultured with microglia showed upregulation of ISGs, and GSEA indicated IFN and JAK/STAT signalling. (**C**) Differential gene expression analysis between T121 spheroids cultured alone vs T121 spheroids cultured with TMZ and microglia showed the same expression profile as co-culturing without TMZ exposure. For both A and C, the 60 and 120 μM TMZ samples were pooled in the analysis, as these groups showed comparable results. Separate analyses can be found in **Figure** S3. Experiments were performed in biological triplicates.

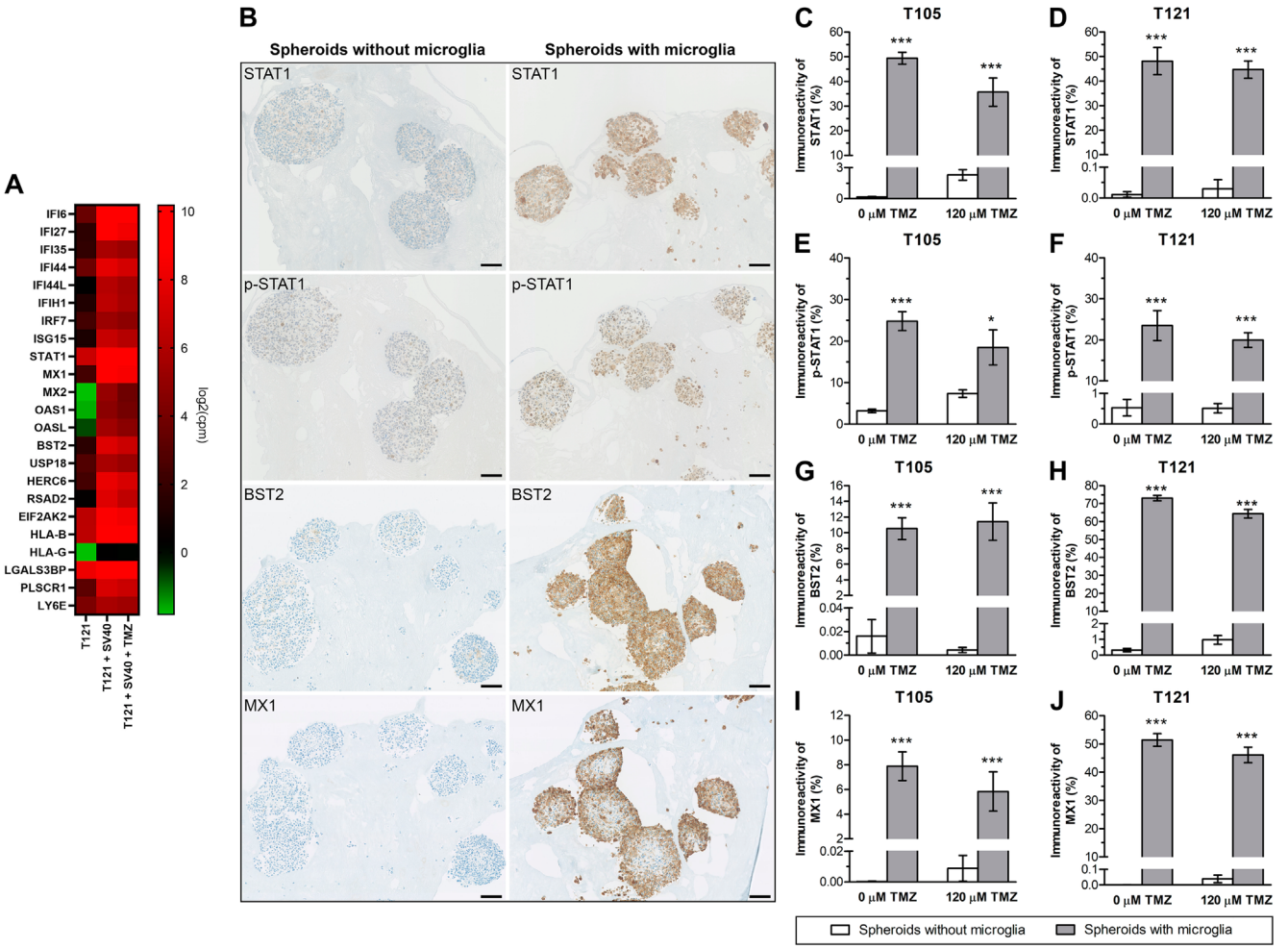

FIGURE 4 STAT1 signalling and IFN-stimulated protein expression levels are upregulated in glioblastoma spheroids after co-culture with microglia. (**A**) Heatmap showing the expression of the most well-described ISGs in T121 spheroids cultured with and without SV40 immortalised microglia and TMZ. (**B**) IHC staining of STAT1, p-STAT1, BST2 and MX1 on paraffin-embedded cell clots from T121 spheroids cultured with (right) and without (left) SV40 microglia. (**C–J**) Immunoreactivity of STAT1 (C, D), p-STAT1 (E, F), BST2 (G, H) and MX1 (I, J) in two glioblastoma cell cultures co-cultured with (grey) and without (white) SV40 microglia and with and without TMZ. The level of significance is indicated with asterisks (* $p < 0.05$; *** $p < 0.005$). SEM based on two biological replicates is indicated by the vertical lines. The scale bar in B is 100 μm.

(**Figure** 4I, J). The immunostaining supports the RNA-seq data and suggests a microglial-induced activation of the STAT1 signalling pathway as well as an upregulation of ISG expression in glioblastoma cells.

Expression of ISGs in glioblastoma correlates with the presence of microglia

To further investigate the association between microglia and ISG expression in glioblastoma, we utilised data from TCGA and CGGA. We analysed if there was a correlation between two known markers of microglia and the top five most differentially expressed ISGs from the RNA-seq analysis (**Figure** S4). Overall, there was a significant positive correlation between the expression of the top five expressed ISGs and *AIF1* and *TMEM119* in both datasets. However, *IFI27* expression only correlated with the expression of the more general TAM marker *AIF1* and not the microglia-specific marker *TMEM119*. Further, *HERC6* had a stronger correlation with *TMEM119* compared with *AIF1*. We also analysed *STAT1* correlation with the microglia markers and found that *STAT1* expression only correlated positively with *TMEM119* and not the general TAM marker *AIF1*. The data suggest a tendency towards a higher expression of ISGs in glioblastomas with higher infiltration levels of microglia. Further, we performed RNA-seq analysis on single-cultured SV40 microglia and SV40 microglia co-cultured with T121 glioblastoma spheroids, and these analyses showed no differential expression of ISGs in the microglia (data not shown). This suggests that the ISG signature is specific for glioblastoma cells that are interacting with microglia.

DISCUSSION

In the present study, we showed that co-culturing microglia and glioblastoma cells protects the glioblastoma cells against TMZ-induced

TABLE 1 Differentially expressed genes in RNA-seq samples.

T121 vs T121 + SV40				T121 vs T121 + SV40 + TMZ			
Genes	Log2 FC	*P*-value	FDR	Genes	Log2 FC	*P*-value	FDR
IFI27	6.21	2.77E-37	1.12E-34	***IFI27***	6.55	2.07E-108	1.40E-104
AC017076.5	5.84	1.03E-44	7.22E-42	***RSAD2***	6.18	2.06E-25	1.04E-22
MX1	5.68	6.97E-24	1.39E-21	***MX1***	6.15	3.80E-80	1.03E-76
RP1-71H24.1	5.20	1.79E-65	7.51E-62	***IFI6***	5.52	3.75E-106	1.70E-102
IFI6	5.11	8.67E-47	7.78E-44	***IFI44L***	5.38	3.73E-11	3.68E-09
BST2	5.09	4.17E-43	2.50E-40	***OASL***	5.33	5.60E-10	4.81E-08
OAS1	5.03	2.10E-22	3.67E-20	***BST2***	5.30	4.57E-116	6.19E-112
HERC6	5.00	2.66E-75	1.67E-71	***ISG15***	5.27	3.40E-30	2.31E-27
RSAD2	4.95	8.09E-12	4.84E-10	***XAF1***	5.13	1.07E-08	7.10E-07
RTP4	4.88	1.96E-35	7.05E-33	***COL3A1***	5.13	0.00136	0.020761
CMPK2	4.84	1.36E-44	8.99E-42	***RP1-71H24.1***	5.02	1.71E-27	1.01E-24
ISG15	4.65	1.53E-18	2.16E-16	***HERC6***	4.95	5.62E-91	1.90E-87
IFI44L	4.37	4.19E-07	1.11E-05	***HERC5***	4.66	7.81E-15	1.47E-12
HERC5	4.30	2.63E-14	2.31E-12	***CMPK2***	4.62	4.87E-33	4.40E-30
MX2	4.25	1.05E-05	0.00019	***DDX60***	4.58	1.90E-36	2.15E-33
IFIH1	4.23	6.18E-24	1.25E-21	***COL1A2***	4.56	0.001824	0.025834
DDX60	4.22	1.15E-25	2.53E-23	***TGFBI***	4.54	0.001038	0.016745
EPSTI1	4.17	3.21E-07	8.73E-06	***IFIH1***	4.50	6.36E-23	2.69E-20
DDX58	3.97	4.43E-56	6.19E-53	***COL6A3***	4.49	0.002099	0.028712
SLC15A3	3.96	5.86E-09	2.29E-07	***PARP12***	3.92	4.34E-36	4.52E-33
OASL	3.93	3.16E-07	8.66E-06	***DDX58***	3.89	4.18E-40	5.67E-37
C19orf66	3.92	8.94E-33	3.12E-30	***SAMD9***	3.81	9.89E-19	3.12E-16
PARP12	3.88	3.28E-50	3.43E-47	***PLSCR1***	3.70	1.30E-43	2.52E-40
SAMD9L	3.78	4.15E-29	1.16E-26	***DDX60L***	3.68	2.04E-30	1.46E-27
DDX60L	3.75	1.06E-39	5.34E-37	***IFI44***	3.61	4.99E-26	2.70E-23

Note: Top 25 differentially expressed genes for T121 vs T121 spheroids co-cultured with SV40 microglia (left) and T121 vs T121 spheroids co-cultured with SV40 microglia and treated with TMZ (right; 60 and 120 μM pooled in analysis), sorted by $\log_2$ fold change.
Abbreviations: FDR, false discovery rate; logFC, log fold change.

cell death (**Figure** 5). We also found that microglia induce expression of ISGs in glioblastoma cells possibly leading to a reduced TMZ sensitivity of the glioblastoma cells. This gene expression signature corresponds to the previously described IRDS, which is upregulated in different cancers and is linked to radiation and chemotherapy resistance [24, 25]. However, we here report for the first time that the IRDS can be induced by microglia. This opens up an alternative therapeutic target to increase the elimination of glioblastoma cells with TMZ, seeing that microglia are genetically stable and possibly easier targetable than the heterogeneous, unstable glioblastoma cells. The IRDS genes identified in our RNA-seq analysis are comparable with the previously observed signature, with highly significant, differential expression of genes including *IFI6*, *IFI27*, *MX1*, *BST2* and *HERC6* in glioblastoma cells following co-culture with microglia. In addition, *STAT1* expression was significantly upregulated indicating JAK/STAT signalling. These results were confirmed at a protein level for STAT1, BST2 and MX1. In data from the TCGA and CGGA, we observed a positive correlation between the most upregulated ISGs and *AIF1*, a pan-marker for TAMs, as well as *TMEM119*, a microglia-specific marker. Furthermore, *STAT1* expression correlated positively with *TMEM119* expression. In our RNA-seq data, we also observed a significant expression of six proposed regulators of the IRDS genes [20]. Using an upstream regulator analysis with ingenuity pathway analysis, Padariya *et al.* suggested *IRF7*, *EIF2AK2*, *STAT1*, *USP18*, *ISG15* and *IFIH1* as major regulators of the IRDS genes. All six proposed regulators were upregulated in glioblastoma cells after co-culture with microglia. Together, this supports the hypothesis that the expression levels of ISGs as well as IFN and STAT1 signalling are elevated in microglia-rich glioblastomas.

Our observed association between microglia and the ISG expression profile as well as TMZ resistance is supported by previous studies. In one study, phosphatidylinositol 3-kinase gamma (PI3Kγ) inhibition in glioblastoma decreased intratumoural microglia infiltration that in turn increased survival and TMZ response in a murine model [44]. In another study, microglia depletion in brain slices resulted in the downregulation of ISGs as well as reduced JAK/STAT

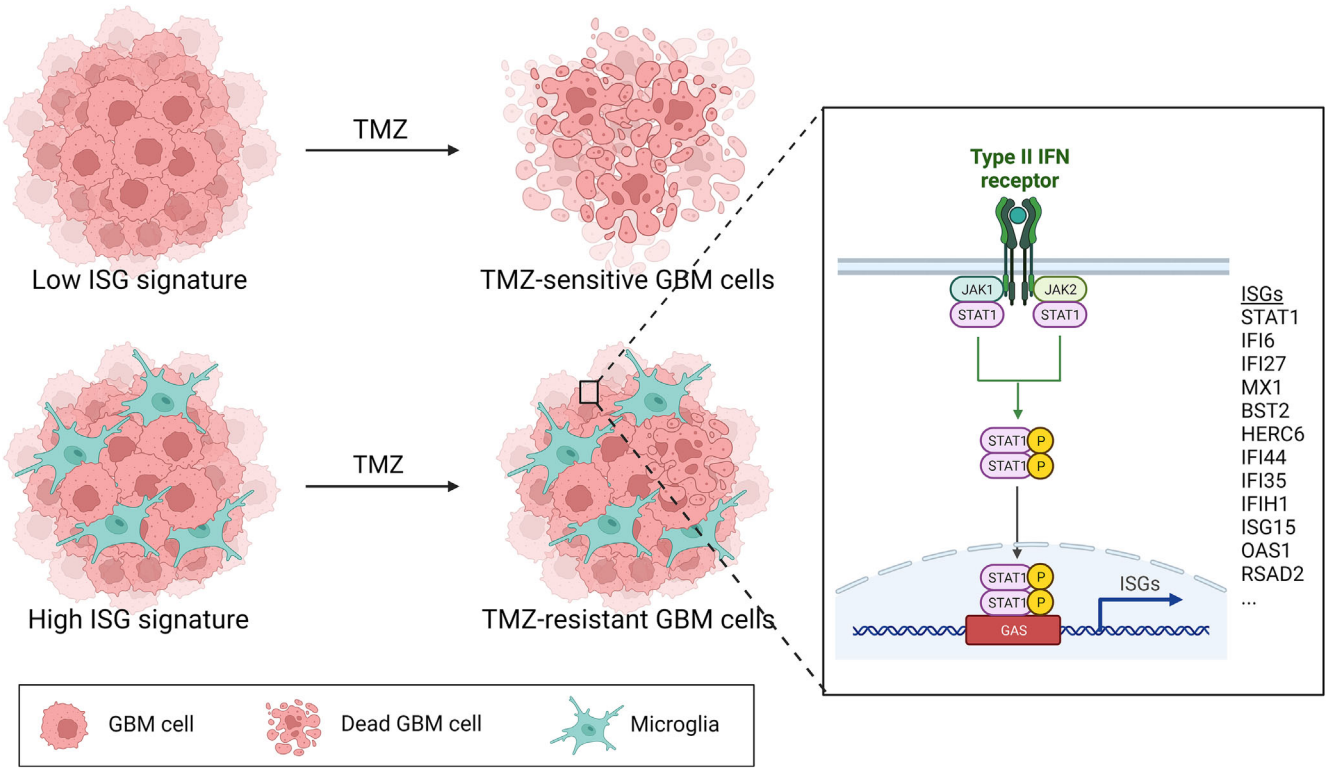

FIGURE 5 A hypothesis for microglial-mediated TMZ resistance in glioblastoma. Glioblastomas with low infiltration of microglia have a low expression of ISGs and are more sensitive to TMZ treatment (top panel), while microglia-rich glioblastomas have high levels of ISGs and show increased resistance to TMZ-induced cell death (bottom panel). Microglia infiltrating glioblastoma stimulate the expression of ISGs, possibly through secretion of IFNs, resulting in STAT1 signalling. Phosphorylation of STAT1 leads to binding of p-STAT1 to gamma-activated sequence (GAS) initiating transcriptional activation of different ISGs [20]. In this way, glioblastoma cells acquire an IFN-related DNA damage resistance signature (IRDS) that protects them against TMZ-mediated cell damage. The illustration was created with BioRender.com.

signalling in astrocytes [45]. In addition, we found that ISG expression correlated with the presence of microglia in glioblastoma using *in silico* datasets. Interestingly, Khan *et al.* reported a significant association between IFN/STAT1 signalling and the mesenchymal phenotype in glioblastoma [46], which is characterised by high TAM infiltration. Further, they showed that high *STAT1* expression correlated with poorer prognosis in the mesenchymal subtype only [46], suggesting a relation between TAMs and the STAT1 pathway. Additionally, IFN/STAT1 signalling and high ISG expression were mainly present in glioblastoma stem-like cells, linking the ISGs to more aggressive glioblastoma cells. In line with these results, Yang *et al.* identified the ISG expression profile in a subpopulation of glioblastoma cells by single-cell sequencing, and this subpopulation actively interacted with TAMs and predicted shorter survival in patients with glioblastoma who had received radio-chemotherapy [25]. Further, we have previously shown that high levels of CD204-positive TAMs correlate with shorter overall survival in glioblastoma [10]. Interestingly, in the group with MGMT methylated tumours, patients whose tumours had high CD204 expression showed a poorer prognosis than patients whose tumours had low CD204 levels. This finding suggests a possible chemo-protective role of TAMs in glioblastoma, supporting our *in vitro* results in the present study. Collectively, these findings indicate that both microglia and the ISG expression profile may correlate with tumour aggressiveness, chemo-resistance and poorer outcome in patients with glioblastoma.

The IRDS genes could be explored as therapeutic targets to eliminate the TMZ-resistant glioblastoma cells. Seeing that these genes are regulated by STAT1, they could be targeted together with a STAT1 inhibitor, for example, fludarabine, which inhibits STAT1 phosphorylation and signalling, potentially leading to downregulation of ISGs [20, 47]. Fludarabine is already approved for haematological malignancies. Bromodomain and extra-terminal domain (BET) inhibitors could also potentially be used to inhibit ISGs. BET proteins are epigenetic regulators of gene transcription, and an *in vitro* study using glioblastoma spheroids suggested that a BET inhibitor could directly inhibit the transcriptional level of ISGs, bypassing STAT1 signalling [48]. In addition, depletion of the IRDS-inducing microglia may be a favourable therapeutic strategy. In this study, we used microglial cell lines to test our hypothesis; however, in an *in vivo* setting, macrophages may also be responsible for the possible ISG-mediated TMZ resistance. The IRDS profile has been observed in other solid cancers, for example, breast and lung cancer [24], and macrophages could potentially play a role here, although this has not been investigated. Thus, additional *in vivo* experiments are needed to elucidate whether the microglia and/or macrophage subpopulation is responsible for the observed effect using, for example, single-cell sequencing and spatial multiomics.

In conclusion, our study show that microglia can promote the development of TMZ-resistant glioblastoma cells via induction of ISG expression. The ISG gene expression signature has been linked to resistance and described as an IRDS. These genes as well as the IRDS-inducing microglia could serve as valuable therapeutic targets in glioblastoma.

AUTHOR CONTRIBUTIONS

Conceptualisation and study design: Mia Dahl Sørensen and Bjarne Winther Kristensen. Data acquisition: Mia Dahl Sørensen, Stephanie Kavan and Stine Asferg Petterson. Data analysis and interpretation: Mia Dahl Sørensen, Rikke Frydendahl Sick Olsen, Mark Burton, Mads Thomassen, Torben Arvid Kruse and Bjarne Winther Kristensen. Reagent/materials/analysis tools: Mia Dahl Sørensen, Morten Meyer and Bjarne Winther Kristensen. Drafting of the manuscript: Mia Dahl Sørensen and Rikke Frydendahl Sick Olsen. Editing of the manuscript: Mia Dahl Sørensen, Rikke Frydendahl Sick Olsen and Bjarne Winther Kristensen. All authors have read and approved the final manuscript.

ACKNOWLEDGEMENTS

We gratefully acknowledge the assistance with the immunostaining by technicians Helle Wohlleben and Lone Christiansen. Parts of the study were based on data generated by the TCGA Research Network, and we thankfully acknowledge all tissue donors and workers involved in the project.

CONFLICT OF INTEREST STATEMENT

The authors declare no conflicts of interest.

PEER REVIEW

The peer review history for this article is available at https://www.webofscience.com/api/gateway/wos/peer-review/10.1111/nan.13016.

DATA AVAILABILITY STATEMENT

The data that supports the findings of this study are available in the supplementary material of this article.

ETHICS STATEMENT

Written informed consent was obtained from all patients, and the Regional Scientific Ethical Committee approved the study (S-20150148).

REFERENCES

1. Stupp R, Mason WP, van den Bent MJ, et al. Radiotherapy plus concomitant and adjuvant temozolomide for glioblastoma. *N Engl J Med*. 2005;352(10):987-996. doi:10.1056/NEJMoa043330
2. Tykocki T, Eltayeb M. Ten-year survival in glioblastoma. A systematic review. *J Clin Neurosci*. 2018;54:7-13. doi:10.1016/j.jocn.2018.05.002
3. Weller M, Stupp R, Reifenberger G, et al. MGMT promoter methylation in malignant gliomas: ready for personalized medicine? *Nat Rev Neurol*. 2010;6:39-51.
4. Hegi ME, Diserens AC, Godard S, et al. Clinical trial substantiates the predictive value of O-6-methylguanine-DNA methyltransferase promoter methylation in glioblastoma patients treated with temozolomide. *Clin Cancer Res*. 2004;10(6):1871-1874. doi:10.1158/1078-0432.CCR-03-0384
5. Hegi ME, Diserens AC, Gorlia T, et al. MGMT gene silencing and benefit from temozolomide in glioblastoma. *N Engl J Med*. 2005;352(10):997-1003. doi:10.1056/NEJMoa043331
6. Hegi ME, Oppong FB, Perry JR, et al. No benefit from TMZ treatment in glioblastoma with truly unmethylated MGMT promoter: reanalysis of the CE.6 and the pooled Nordic/NOA-08 trials in elderly glioblastoma patients. *Neuro Oncol*. 2024;26(10):1867-1875. doi:10.1093/neuonc/noae108
7. Annavarapu S, Gogate A, Pham T, Davies K, Singh P, Robert N. Treatment patterns and outcomes for patients with newly diagnosed glioblastoma multiforme: a retrospective cohort study. *CNS Oncol*. 2021;10(3):Cns76. doi:10.2217/cns-2021-0007
8. Morantz RA, Wood GW, Foster M, Clark M, Gollahon K. Macrophages in experimental and human brain tumors. Part 2: studies of the macrophage content of human brain tumors. *J Neurosurg*. 1979;50(3):305-311. doi:10.3171/jns.1979.50.3.0305
9. Badie B, Schartner JM. Flow cytometric characterization of tumor-associated macrophages in experimental gliomas. *Neurosurgery*. 2000;46(4):957-962. doi:10.1227/00006123-200004000-00035
10. Hambardzumyan D, Gutmann DH, Kettenmann H. The role of microglia and macrophages in glioma maintenance and progression. *Nat Neurosci*. 2016;19(1):20-27. doi:10.1038/nn.4185
11. Sorensen MD, Dahlrot RH, Boldt HB, et al. Tumour-associated microglia/macrophages predict poor prognosis in high-grade gliomas and correlate with an aggressive tumour subtype. *Neuropathol Appl Neurobiol*. 2018;44(2):185-206. doi:10.1111/nan.12428
12. Andersen RS, Anand A, Harwood DSL, Kristensen BW. Tumor-associated microglia and macrophages in the glioblastoma microenvironment and their implications for therapy. *Cancers (Basel)*. 2021;13(17):13. doi:10.3390/cancers13174255
13. Liu S, Zhang C, Maimela NR, et al. Molecular and clinical characterization of CD163 expression via large-scale analysis in glioma. *Onco Targets Ther*. 2019;8(7):1601478. doi:10.1080/2162402X.2019.1601478
14. Sa JK, Chang N, Lee HW, et al. Transcriptional regulatory networks of tumor-associated macrophages that drive malignancy in mesenchymal glioblastoma. *Genome Biol*. 2020;21(1):216. doi:10.1186/s13059-020-02140-x
15. Bhat KPL, Balasubramaniyan V, Vaillant B, et al. Mesenchymal differentiation mediated by NF-κB promotes radiation resistance in glioblastoma. *Cancer Cell*. 2013;24(3):331-346. doi:10.1016/j.ccr.2013.08.001
16. Wang Q, Hu B, Hu X, et al. Tumor evolution of glioma-intrinsic gene expression subtypes associates with immunological changes in the microenvironment. *Cancer Cell*. 2017;32(1):42-56.e6. doi:10.1016/j.ccell.2017.06.003
17. Di Ianni N, Maffezzini M, Eoli M, et al. Revisiting the immunological aspects of temozolomide considering the genetic landscape and the immune microenvironment composition of glioblastoma. *Front Oncol*. 2021;11:747690. doi:10.3389/fonc.2021.747690
18. Li Z, Meng X, Wu P, et al. Glioblastoma cell-derived lncRNA-containing exosomes induce microglia to produce complement C5 promoting chemotherapy resistance. *Cancer Immunol Res*. 2021;9(12):1383-1399. doi:10.1158/2326-6066.CIR-21-0258
19. Liu X, Huang Y, Qi Y, et al. The GBM tumor microenvironment as a modulator of therapy response: ADAM8 causes tumor infiltration of tams through HB-EGF/EGFR-mediated CCL2 expression and overcomes TMZ Chemosensitization in glioblastoma. *Cancers (Basel)*. 2022;14(19):4910. doi:10.3390/cancers14194910
20. Padariya M, Sznarkowska A, Kote S, et al. Functional interfaces, biological pathways, and regulations of interferon-related DNA damage resistance signature (IRDS) genes. *Biomolecules*. 2021;11(5):622. doi:10.3390/biom11050622

21. Gavish A, Tyler M, Greenwald AC, et al. Hallmarks of transcriptional intratumour heterogeneity across a thousand tumours. *Nature*. 2023; 618(7965):598-606. doi:10.1038/s41586-023-06130-4
22. Qadir AS, Ceppi P, Brockway S, et al. CD95/Fas increases stemness in cancer cells by inducing a STAT1-dependent type I interferon response. *Cell Rep*. 2017;18(10):2373-2386. doi:10.1016/j.celrep.2017.02.037
23. Benci JL, Xu B, Qiu Y, et al. Tumor interferon signaling regulates a multigenic resistance program to immune checkpoint blockade. *Cell*. 2016;167(6):1540-1554.e12. doi:10.1016/j.cell.2016.11.022
24. Weichselbaum RR, Ishwaran H, Yoon T, et al. An interferon-related gene signature for DNA damage resistance is a predictive marker for chemotherapy and radiation for breast cancer. *Proc Natl Acad Sci U S a*. 2008;105(47):18490-18495. doi:10.1073/pnas.0809242105
25. Yang K, Shi Y, Luo M, et al. Identification of a unique tumor cell subset employing myeloid transcriptional circuits to create an immunomodulatory microenvironment in glioblastoma. *Onco Targets Ther*. 2022;11(1):2030020. doi:10.1080/2162402X.2022.2030020
26. Kolenda J, Jensen SS, Aaberg-Jessen C, et al. Effects of hypoxia on expression of a panel of stem cell and chemoresistance markers in glioblastoma-derived spheroids. *J Neurooncol*. 2011;103(1):43-58. doi:10.1007/s11060-010-0357-8
27. Munthe S, Sorensen MD, Thomassen M, et al. Migrating glioma cells express stem cell markers and give rise to new tumors upon xenografting. *J Neurooncol*. 2016;130(1):53-62. doi:10.1007/s11060-016-2221-y
28. Aaberg-Jessen C, Norregaard A, Christensen K, et al. Invasion of primary glioma- and cell line-derived spheroids implanted into corticostriatal slice cultures. *Int J Clin Exp Pathol*. 2013;6(4):546-560.
29. Knudsen AM, Halle B, Cédile O, et al. Surgical resection of glioblastomas induces pleiotrophin-mediated self-renewal of glioblastoma stem cells in recurrent tumors. *Neuro Oncol*. 2022;24(7):1074-1087. doi:10.1093/neuonc/noab302
30. Verhaak RGW, Hoadley KA, Purdom E, et al. An integrated genomic analysis identifies clinically relevant subtypes of glioblastoma characterized by abnormalities in PDGFRA, IDH1, EGFR and NF1. *Cancer Cell*. 2010;17(1):98-110. doi:10.1016/j.ccr.2009.12.020
31. Zacher A, Kaulich K, Stepanow S, et al. Molecular diagnostics of gliomas using next generation sequencing of a glioma-tailored gene panel. *Brain Pathol*. 2017;27(2):146-159. doi:10.1111/bpa.12367
32. Blasi E, Barluzzi R, Bocchini V, Mazzolla R, Bistoni F. Immortalization of murine microglial cells by a v-raf/v-myc carrying retrovirus. *J Neuroimmunol*. 1990;27(2-3):229-237. doi:10.1016/0165-5728(90)90073-V
33. Schmidt SI, Bogetofte H, Ritter L, et al. Microglia-secreted factors enhance dopaminergic differentiation of tissue- and iPSC-derived human neural stem cells. *Stem Cell Rep*. 2021;16(2):281-294. doi:10.1016/j.stemcr.2020.12.011
34. Janabi N, Peudenier S, Héron B, Ng KH, Tardieu M. Establishment of human microglial cell lines after transfection of primary cultures of embryonic microglial cells with the SV40 large T antigen. *Neurosci Lett*. 1995;195(2):105-108. doi:10.1016/0304-3940(94)11792-H
35. Nørregaard A, Jensen SS, Kolenda J, et al. Effects of chemotherapeutics on organotypic corticostriatal slice cultures identified by a panel of fluorescent and immunohistochemical markers. *Neurotox Res*. 2012;22(1):43-58. doi:10.1007/s12640-011-9300-9
36. Schneider CA, Rasband WS, Eliceiri KW. NIH image to ImageJ: 25 years of image analysis. *Nat Methods*. 2012;9(7):671-675. doi:10.1038/nmeth.2089
37. Sorensen MD, Kristensen BW. Tumour-associated CD204(+) microglia/macrophages accumulate in perivascular and perinecrotic niches and correlate with an interleukin-6-enriched inflammatory profile in glioblastoma. *Neuropathol Appl Neurobiol*. 2022;48(2): e12772. doi:10.1111/nan.12772
38. Bushnell B, Rood J, Singer E. BBMerge—accurate paired shotgun read merging via overlap. *PLoS ONE*. 2017;12(10):e0185056. doi:10.1371/journal.pone.0185056
39. Kim D, Pertea G, Trapnell C, Pimentel H, Kelley R, Salzberg SL. TopHat2: accurate alignment of transcriptomes in the presence of insertions, deletions and gene fusions. *Genome Biol*. 2013;14(4):R36. doi:10.1186/gb-2013-14-4-r36
40. Anders S, Pyl PT, Huber W. HTSeq—a Python framework to work with high-throughput sequencing data. *Bioinformatics*. 2015;31(2): 166-169. doi:10.1093/bioinformatics/btu638
41. Robinson MD, McCarthy DJ, Smyth GK. edgeR: a Bioconductor package for differential expression analysis of digital gene expression data. *Bioinformatics*. 2010;26(1):139-140. doi:10.1093/bioinformatics/btp616
42. Subramanian A, Kuehn H, Gould J, Tamayo P, Mesirov JP. GSEA-P: a desktop application for gene set enrichment analysis. *Bioinformatics*. 2007;23(23):3251-3253. doi:10.1093/bioinformatics/btm369
43. Bowman RL, Wang Q, Carro A, Verhaak RGW, Squatrito M. GlioVis data portal for visualization and analysis of brain tumor expression datasets. *Neuro Oncol*. 2017;19(1):139-141. doi:10.1093/neuonc/now247
44. Li J, Kaneda MM, Ma J, et al. PI3Kγ inhibition suppresses microglia/TAM accumulation in glioblastoma microenvironment to promote exceptional temozolomide response. *Proc Natl Acad Sci U S a*. 2021;118(16):e2009290118. doi:10.1073/pnas.2009290118
45. Henrik Heiland D, Ravi VM, Behringer SP, et al. Tumor-associated reactive astrocytes aid the evolution of immunosuppressive environment in glioblastoma. *Nat Commun*. 2019;10(1):2541. doi:10.1038/s41467-019-10493-6
46. Khan S, Mahalingam R, Sen S, et al. Intrinsic interferon signaling regulates the cell death and mesenchymal phenotype of glioblastoma stem cells. *Cancers (Basel)*. 2021;13(21):5284. doi:10.3390/cancers13215284
47. Feng Z, Zheng W, Tang Q, et al. Fludarabine inhibits STAT1-mediated up-regulation of caspase-3 expression in dexamethasone-induced osteoblasts apoptosis and slows the progression of steroid-induced avascular necrosis of the femoral head in rats. *Apoptosis*. 2017;22(8):1001-1012. doi:10.1007/s10495-017-1383-1
48. Gusyatiner O, Bady P, Pham MDT, et al. BET inhibitors repress expression of interferon-stimulated genes and synergize with HDAC inhibitors in glioblastoma. *Neuro Oncol*. 2021;23(10):1680-1692. doi:10.1093/neuonc/noab115

SUPPORTING INFORMATION

Additional supporting information can be found online in the Supporting Information section at the end of this article.

How to cite this article: Sørensen MD, Olsen RFS, Burton M, et al. Microglia induce an interferon-stimulated gene expression profile in glioblastoma and increase glioblastoma resistance to temozolomide. *Neuropathol Appl Neurobiol*. 2024; 50(6):e13016. doi:10.1111/nan.13016